Equilibria and Kinetics of some Metal Complexes of Peptide Hydroxamic Acids

C. ALLEN CHANG*, V. CHANDRA SEKHAR, B. S. GARG

Department of Chemistry, University of Texas at El Paso, El Paso, Tex. 79968, U.S.A.

FRANK S. GUZIEC, Jr. and TERESA CARRERA RUSSO

Department of Chemistry, New Mexico State University, Las Cruces, N.M. 88003, U.S.A.

(Received May 9, 1986; revised July 16, 1986)

Abstract

The complex formation constants of a number of metal ions with a few peptide hydroxamic acid ligands were determined using either a spectrophotometric or a potentiometric method. They are in general lower than those of acetohydroxamic acid complexes due to the lower pK_a values of these peptide hydroxamic acids. No cooperative effect was found for any of the metal–peptide hydroxamate complexes indicating that peptide chain interaction is probably not significant in solution. The Fe(III)/Z-Ala-Gly-NHOH complexes do not form any precipitate up to pH ~10 which may be due to well shielded solution structures. The kinetics of dissociation of $[Fe(Z\text{-}Gly\text{-}NHO)]^{2+}$ complex were studied at a constant ionic strength of 1.0 ($NaClO_4$), in the 2.5×10^{-2} M to 1.0 M acid concentration range. The complex exhibits both acid-dependent and acid-independent parallel pathways leading to dissociation. At low acid concentration the $[Fe(Z\text{-}Gly\text{-}NHO)OH]^{+}$ species dominates in solution and is more reactive than the unhydrolyzed species towards ligand loss. Activation parameters were obtained for both acid independent and acid-dependent pathways from the temperature dependence of rate-constants in the 15 to 35 °C range. The enthalpy and entropy of activation for acid-independent and acid-dependent paths are 16.6 ± 0.4 kcal/mol and -6.5 ± 1.3 e.u.; and 10.2 ± 2.0 kcal/mol and -29.6 ± 8.0 e.u., respectively.

Introduction

There has been a great deal of interest in recent years concerning the chemistry of hydroxamic acid derivatives due to their biological significance, analytical and industrial applications. For example, along with amino acids, peptide hydroxamic acids have been widely investigated as inhibitors of proteolytic enzymes. Some of these compounds have proved to be potent inhibitors of thermolysin [1, 2], elastase [3] and aminopeptidases [4, 5]. These enzymes are metalloproteases and the mechanism of inhibition appears to involve chelation of metals at their active sites. It is also known that hydroxamic acid moiety is a constituent of antibiotics, tumor inhibitors, antifungal agents, food additives and growth factors; and its derivatives are widely used in nuclear fuel processing, extractive metallurgy and in inhibition of copper corrosion [6–16].

More recently, interest in this class of compounds has been growing mainly due to the fact that they are capable of binding Fe(III) selectively among a number of physiologically important metal ions. Certain naturally occurring hydroxamic acids are involved in microbial transport of iron and are named as siderophores [17]. Synthesized hydroxamic acids show remarkable specificity for Fe(III) and the tris-(hydroxamato)Fe(III) complexes have very large stability constants [18] ($\log K$ around 30). Although a lot of work has been done on their synthesis and structural characterization, relatively fewer papers have appeared dealing with the solution equilibria of metal complexes of hydroxamic acids and the volume of kinetic and mechanistic work done on these systems is minute by comparison [19]. It would be quite interesting to know if the substituents on the hydroxamic acids have any effect on the stabilities of their metal complexes. Also their dissociation kinetics is of special importance because of its implications in understanding the mechanism of Fe(III) removal from the naturally occurring compounds containing iron–hydroxamate moiety, such as siderophores.

In continuation of our recent efforts to understand the thermodynamic stabilities of metal complexes containing polydentate ligands and as a part of our ongoing research program [20, 21], we have undertaken a potentiometric and spectrophotometric study of several transition metal complexes of substituted peptide hydroxamic acids (Fig. 1). Also investigated using a stopped-flow method are the rate

*Author to whom correspondence should be addressed.

0020-1693/87/$3.50

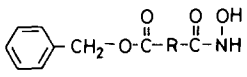

R	Abbreviation
1. $-NHCH_2-$	Z-Gly-NHOH
2. $-NHCH(CH_3)C(=O)NHCH_2-$	Z-Ala-Gly-NHOH
3. $-NHCH(CH(CH_3)_2)-$	Z-Val-NHOH
4. $-NHCH(CH_2C_6H_5)-$	Z-Phe-NHOH
5. $-NHCH_2C(=O)NHCH(CH_2CH(CH_3)_2)-$	Z-Gly-Leu-NHOH

Fig. 1. Structural formulae of peptide hydroxamic acids of interest.

and mechanism of acid-catalyzed dissociation of an Fe(III) complex. We wish to report here the results obtained during the course of this investigation.

Experimental

Synthesis of Peptide Hydroxamic Acids

The hydroxamic acids were prepared by modifications of the methods of Hoffman and Faiferman [22]. Hydroxaminolysis of protected amino acid or peptide esters in general appears to be the most convenient method for hydroxamic acid preparation. In cases where the C-terminal amino acid was bulky, a modified mixed anhydride procedure was used for the hydroxamic acid synthesis.

Melting points were determined using a Mel-Temp capillary block apparatus and are uncorrected. ^1H NMR spectra were recorded using a Varian XL 200 spectrometer with tetramethylsilane as an internal standard. IR spectra were recorded on a Perkin-Elmer 283 spectrophotometer. Elemental analyses were performed by Galbraith Laboratories, Knoxville, Tenn. Solvents were removed using a rotary evaporator under reduced pressure. All hydroxamic acids gave a characteristic purple color in the presence of ferric ion. Protected amino acids were obtained from Sigma Chemical Company, St. Louis, Mo. Protected peptide derivatives were prepared using water-soluble carbodiimide and had the expected physical and spectroscopic properties.

Hydroxylaminolysis Method

N-Benzyloxycarbonylglycyl hydroxamic acid (1)

Hydroxylamine hydrochloride (2.0 g, 28 mmol) was dissolved in hot methanol (~5 ml) and the resulting solution cooled to 30–40 °C, avoiding excessive exposure to air. A solution of potassium hydroxide (1.1 g, 20 mmol) in ~3 ml methanol was added and the mixture allowed to stand in an ice bath for 5 min. *N*-benzyloxycarbonylglycine methyl ester (2.9 g, 14.2 mmol) was added and the resulting mixture allowed to stand at room temperature for 48 h at which time TLC indicated no starting material was present. The solution was concentrated at room temperature and acidified to pH ~2 with 2 M HCl, at which time colorless crystals of the hydroxamic acids separated. Cooling and filtering afforded the crude hydroxamic acid **1**, 2.7 g, 93% yield, melting point (m.p.) 109–111 °C. ^1H NMR ($CDCl_3$): δ 8.8(bs, 1H), 7.34(s, 5H), 6.7(bm, 1H), 5.10(s, 2H), 3.82(d, 2H), 3.04(s, 1H) (the signals at δ 8.8 and 3.04 rapidly exchange with D_2O). IR (KBr) 3320, 3158, 1690, 1670 cm^{-1}. Recrystallization from dioxane–toluene afforded material melting 118–120 °C (literature 118–120 °C [22]).

N-Benzyloxycarbonyl–L-alanylglycyl hydroxamic acid (2)

This peptide hydroxamic acid was prepared on a 6.8 mmol scale according to the procedure outlined for the preparation of **1** affording a colorless solid. Two recrystallizations from ethanol–hexanes afforded colorless crystals of **2**, (0.45 g, 22% yield), m.p. 143–144 °C (literature 140 °C [6]). ^1H NMR ($CDCl_3$–DMSO-d_6): δ 8.84(bs, 1H), 8.0(bt, 1H), 7.34(s, 5H), 7.2(bd, 1H), 5.09(s, 2H), 4.3–4.1(m, 1H), 4.0–3.7(m, 2H), 3.21(s, 1H), 1.28(d, 3H) (the signals at δ 8.84 and 3.21 rapidly exchange with D_2O). IR (KBr): 3310, 3260, 1685, 1650, 1535, 1260, 1240 cm^{-1}.

Mixed Anhydride Method

N-Benzyloxycarbonyl–L-valyl hydroxamic acid (3)

N-Benzyloxycarbonylvaline (2.51 g, 10 mmol) and *N*-methylpiperidine (0.99 g, 1.2 ml, 10 mmol) in dichloromethane (20 ml) at −5 °C was treated with isobutyl chloroformate (1.36 g, 1.3 ml, 10 mmol) and the solution allowed to stir at −5 °C for 5 min. A solution of hydroxylamine hydrochloride (0.70 g, 10 mmol) and sodium hydroxide (0.40 g, 10 mmol) in methanol (8 ml) was added dropwise and the mixture allowed to stand at room temperature overnight.

The mixture was concentrated at room temperature and the residue taken up in ether and 2 M HCl. The ether phase was dried and concentrated and the residue was recrystallized from ethanol–hexanes affording 0.38 g of colorless crystals, m.p. 155 °C. ^1H NMR ($CDCl_3$–DMSO-d_6): δ 8.72(bs, 1H), 7.38(s, 5H), 6.10(d, 1H), 5.10(s, 1H), 5.09(s, 1H), 3.97(d, 1H), 2.90(bs, 1H), 2.06(septet, 1H), 0.95(d, J = 7 Hz,

3H), 0.93(d, J = 7 Hz, 3H). IR (KBr): 3340, 3240, 1685(sh), 1650, 1550, 1540 cm^{-1}. *Anal.* Calc. for $C_{13}H_{18}N_2O_4$: C, 58.63; H, 6.81; N, 10.52. Found: C, 58.85; H, 6.95; N, 10.73%.

N-Benzyloxycarbonyl-L-phenylalanyl hydroxamic acid (4)

This compound was prepared analogously to the preparation of **3** on a 13.4 mmol scale allowing 48 h for the reaction. After workup and recrystallization from chloroform, colorless crystals (0.54 g, 12%) of hydroxamic acid **4** were obtained, m.p. 140–142 °C. ^1H NMR ($CDCl_3$): δ 8.64(bs, 1H), 7.4–7.2(m, 10H), 6.10(d, 1H), 5.04(s, 2H), 4.42(m, 1H), 3.2–2.9(m, 3H). IR (KBr): 3315, 3250, 3060, 1705(sh), 1685, 1645, 1605, 1530 cm^{-1}. *Anal.* Calc. for $C_{17}H_{18}N_2O_4$: C, 64.95; H, 5.77; N, 8.91. Found: C, 64.76; H, 5.83; N, 9.13%.

N-Benzyloxycarbonylglycyl-L-leucyl hydroxamic acid (5)

This dipeptide hydroxamic acid was prepared on a 5 mmol scale using the mixed anhydride method analogous to the preparation of **3** affording a colorless foam. Recrystallization from ethyl acetate–pentane afforded **5** as colorless crystals (240 mg, 14% yield), m.p. 116–119 °C. ^1H NMR ($CDCl_3$): δ 7.5(bs, 1H), 7.34(s, 5H), 7.08(d, 1H), 6.2(bs, 1H), 6.04(bs, 1H), 5.10(s, 2H), 4.7–4.4(m, 1H), 4.0–3.7(m, 2H), 1.7–1.5(m, 3H), 0.90(brs, 6H). IR (KBr): 3320, 3065, 2960, 1735, 1685, 1660, 1650, 1645, 1635, 1560 cm^{-1}.

Materials and Solutions

Reagent grade chemicals were used without further purification. The stock acid solution of Fe^{3+} was prepared by dissolving anhydrous Fe_2O_3 in stoichiometric amount of analytical grade perchloric acid. All other metal salt (nitrates or chlorides) solutions were prepared and standardized using standard analytical procedures [20].

Potentiometric Titrations

The equilibrium studies were performed by potentiometric titrations using a Fisher 825MP pH meter and a combination pH electrode. All titration solutions were prepared to have a total volume of 25.0 ml and thermostated at 25.0 ± 0.2 °C using a VWR circulating constant temperature water bath. The ionic strength was kept at 0.1 with KNO_3. A water-jacketed titration vessel was used at a constant temperature of 25.0 °C in a similar way as described in our published work [20, 21].

For a typical titration process, the following solutions were prepared:

(i) 2 ml 0.01365 M HNO_3 + 2.5 ml 1 M KNO_3.

(ii) 2 ml 0.01365 M HNO_3 + 2.5 ml 1 M KNO_3 + 5 ml 0.01 M hydroxamic acid.

(iii) 2 ml 0.01365 M HNO_3 + 2.5 ml 1 M KNO_3 + 5 ml 0.01 M hydroxamic acid + 1 ml 0.01 M metal salt solution.

All these solutions were then raised to a final total volume of 25.0 ml by adding reagent grade water (18 Ω) prepared using a Millipore Milli-Q water purification system. Each solution was then titrated against a standard NaOH solution in a nitrogen atmosphere.

Using the titration curves obtained from solutions (i), (ii), and (iii), the average ligand complexation number, $\bar{n}$, and pL (≡ $-\log[L]$, [L] = free ligand concentration) values have been calculated by the procedure of Irving and Rossotti [23]. From the values of $\bar{n}$ and pL, the overall stability constants have been evaluated using the weighed least-squares method of Sullivan *et al.* [24].

Spectroscopic and Kinetic Measurements

These measurements were performed only for Fe(III) complexes. In particular, a spectrophotometric method was followed to determine the formation constants of the Fe(III)(Z-Gly-NHOH) complexes using a Cary Model 118 spectrophotometer with a pair of matched quartz cells. The kinetic studies of dissociation of Fe(III)–Z-Gly-hydroxamic acid complex were performed on a Durrum-Dionex stopped-flow spectrophotometer interfaced with an OLIS computer system.

The complex solution for kinetic studies was made *in situ* by mixing appropriate amounts of Fe^{3+} and ligand solutions (in 1:1 ratio) and adjusting the pH to 3.0. Reactions were monitored by the decrease in the absorbance of complex at 480 nm. Solutions in drive syringes and reaction cell were thermostated at desired temperature (maintained to ±0.2 °C) using a Lauda-Brinkman (Model K-21RD) refrigerated water-bath in combination with a heat exchanger. Reactions were generally followed to 3–5 half lives and A_∞ was taken after 9 half-lives of reactions. Plots of $\log(A_t - A_\infty)$ against time were linear for at least three half-lives of reaction. Observed rate-constants quoted represent the average values of at least three kinetic runs and are reproducible to within ±5%. Errors in rate constants obtained at 45 °C are slightly higher.

Results and Discussion

Spectrophotometric Studies

The spectrophotometric method of McBryde [25, 26] has been used for studying the following equilibria:

$$FeL_{n-1}^{(3-n+1)+} + HL \overset{Q_n}{\rightleftharpoons} FeL_n^{(3-n)+} + H^+ \qquad (1)$$

$n = 1, 2, 3$

This method is adopted because the equilibrium (1) lies far to the right and the normal potentiometric

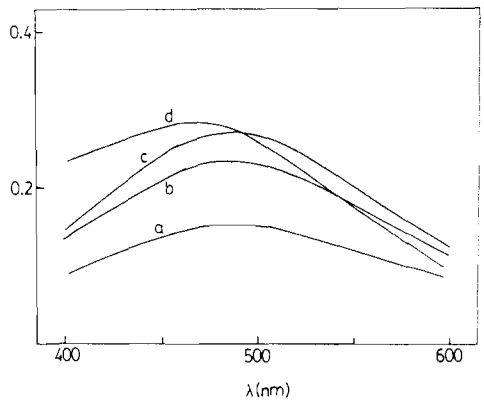

Fig. 2. Aqueous solution absorption spectra of 5×10^{-4} M $[Fe(Z\text{-}Gly\text{-}NHO)]^{2+}$ complex at different pH. (a) pH = 1.57; (b) pH = 2.08; (c) pH = 2.42; (d) pH = 3.05. T = 25 °C.

method is not valid when $n = 1$. Figure 2 shows the spectra of a 1:1 Fe(III)/Z-Gly-NHOH solution at several different pH values. It is seen that the intensity of the absorption band (λ_{max} = 485 nm) increases as the pH is increased, indicating enhanced complex concentration. When pH = 3.05, the spectral band maximum shifts to 475 nm indicating the formation of a different species presumably the hydroxy complex, $[Fe(Z\text{-}Gly\text{-}NHO)(OH)]^{+}$.

When the spectra of solutions containing ligand to metal molar ratio 5:1 were measured at different pH values, similar observations were found. Moreover, from these absorbance values, one can calculate the extinction coefficient on the basis of total metal concentration:

$$\epsilon_M = \epsilon_0\alpha_0 + \epsilon_1\alpha_1 + \epsilon_2\alpha_2 + \epsilon_3\alpha_3$$

where ϵ and α are the respective molar absorptivity and fraction of the metal species. The subscripts 0, 1, 2, 3 denote M, ML, ML_2, and ML_3 species, respectively. Figure 3 shows the plot of ϵ_M values obtained at various pH. The major metal species present at each pH region can therefore be deduced, *i.e.* M + ML (pH < 2.2); ML (2.2 < pH < 3.2); ML + ML_2 (3.2 < pH < 3.7); ML_2 + ML_3 (3.7 < pH < 4.0); ML_3 (pH > 4.0). By choosing ϵ_M values at pH 2.2 (α_1 = 1), 3.5 (α_2 = 1), and 6.5 (α_3 = 1) one can calculate values of ϵ_1, ϵ_2, ϵ_3 at any chosen wavelength (Table I). The value of ϵ_0 is zero in the range of wavelength investigated, *i.e.* λ = 400–600 nm. Equilibrium constant, Q_n, can then be calculated by the expression:

$$Q_n = A_n \frac{[H^+]}{[HL]}$$

where

$$A_n = \frac{[ML_n]}{[ML_{n-1}]} = \frac{\epsilon_{n-1} - \epsilon_M}{\epsilon_M - \epsilon_M}$$

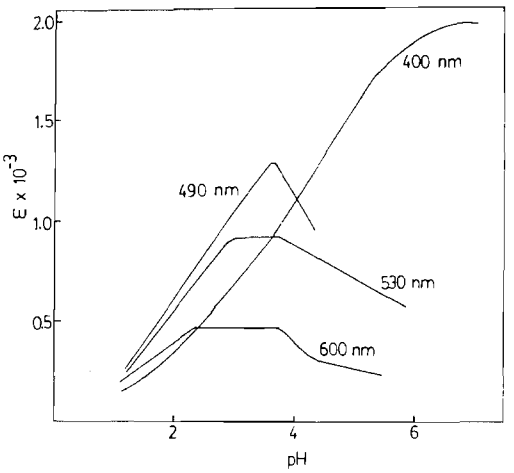

Fig. 3. Variation of molar extinction coefficient for Fe(III)–Z-Gly-NHOH solutions as function of pH (adjusted by adding either HNO_3 or NaOH). $[Fe^{3+}] = 2 \times 10^{-4}$ M, [Z-Gly-NHOH] = 1.0×10^{-3} M; μ = 0.1 (KNO_3), T = 25 °C.

TABLE I. Selected Values of ϵ_n (n = 1, 2, 3) at Several Wavelengths for Fe(III)/Z-Gly-NHOH Complex System

λ (nm)	ϵ_1 (M^{-1} cm^{-1}) (pH = 2.5)	ϵ_2 (M^{-1} cm^{-1}) (pH = 3.5)	ϵ_3 (M^{-1} cm^{-1}) (pH = 6.5)
600	500	500	–
530	735	950	–
400	470	950	2010

and

$$[HL] = ([HL]_{total} - \bar{n}C_M) \Big/ \left(1 + \frac{K_a}{[H^+]}\right)$$

$$\bar{n} = (n - 1) + \alpha_n$$

To calculate Q_1, the quantity

$$A_1 = \frac{[ML]}{[M]}$$

where [M] includes free Fe^{3+} and the hydrolyzed $Fe(OH)^{2+}$ species.

A separate value for the equilibrium constant was obtained from each measurement of optical density subjected to restriction that A_n falls between 0.1 and 10. The stability constant was calculated from the relation:

$$\log K_n = \log Q_n + pK_a$$

or

$$\log K_n = \log A_n - pH + pHL + pK_a$$

TABLE II. Logarithmic Stability Constants of some Metal Complexes of Substituted Hydroxamic Acids[a]

Metal ion	Ligand											
	$CH_3CONHOH$[b]			Z-Gly-NHOH			Z-Val-NHOH			Z-Ala-Gly-NHOH		
	$\log \beta_1$	$\log \beta_2$	$\log \beta_3$	$\log \beta_1$	$\log \beta_2$	$\log \beta_3$	$\log \beta_1$	$\log \beta_2$	$\log \beta_3$	$\log \beta_1$	$\log \beta_2$	$\log \beta_3$
H^+	9.36			8.90			8.43			8.32		
Mn^{2+}	4.0	6.9	–	3.7	5.9	–	–			–		
Fe^{3+}	11.4	21.1	28.3	11.4	21.5	30.2[c]	–			–		
Co^{2+}	5.1	8.9	–	4.2	–	–	4.6	6.8	–	–		
Ni^{2+}	5.3	9.3	–	4.9	7.9	10.9	–			4.1	7.3	–
Cu^{2+}	7.9	–	–	7.1	13.4	–	–			7.0	–	–
Zn^{2+}	5.4	9.6	–	4.7	8.6	–	4.8	8.2	–	4.0	–	–
Cd^{2+}	4.5	7.8	–	4.2	–	–	–			–		
UO_2^{2+}	–			7.6	14.2	–	6.7	12.1	–	6.4	12.4	–
Pb^{2+}	6.7	10.7	–	6.7	11.0	16.3	5.8	–	–	5.8	9.3	–
In^{3+}	9.2	18.4	26.3[d]	7.2	15.2	–	–			–		
Th^{4+}	10.4	20.3	29.3[d]	9.1	–	–						

[a]Standard deviation, ± 0.2 log unit. [b]Data taken from ref. 32. [c]Data obtained by spectrophotometric method. [d]Data obtained for *N*-phenybenzohydroxamic acid, ref. 32, p. 302.

Potentiometric Studies

The calculated values of stability constants of metal complexes of several peptide hydroxamic acids and the pK_a values of these hydroxamic acids are summarized in Table II. For comparison purpose, the values corresponding to the acetylhydroxamic acid are also listed.

A comparison of the stability constants of metal complexes of acetylhydroxamic acid with those of peptide hydroxamic acids indicates that in general, the metal–peptide hydroxamate complexes are weaker. This at least in part is related to the fact that all the peptide hydroxamic acids have lower pK_a values than that of acetylhydroxamic acid.

Among the five peptide hydroxamic acids, neither Z-phe-NHOH nor Z-Gly-Leu-NHOH has sufficient solubility in water to warrant reliable studies. For the remaining three hydroxamic acids, data have been collected mostly for Z-Gly-NHOH. It is found that with most divalent transition and post-transition metal ions, Z-Gly-NHOH, Z-Val-NHOH, and Z-Ala-Gly-NHOH all form complexes of moderate stability. However, their complexes with metal ions of higher charge, *i.e.* +3 or +4, are more stable with Fe(III) forming the most stable complex.

One of the several goals of this study is to examine if there is any cooperative effect among the peptide pendant groups which may reinforce the second and third binding of the ligand. It turns out that the stepwise formation constants are always in the order $K_1 > K_2 > K_3$ for all metal complexes indicating that even if there is positive interaction between the phenyl or peptide side groups, it is not strong enough to facilitate stronger binding of additional ligands.

An interesting observation is made in case of Fe(III)/Z-Ala-Gly-NHOH complexes, for which there is no precipitate formation up to pH ~ 10. Other Fe(III) peptide hydroxamate complexes precipitate out at pH > 6 presumably due to the hydrolysis. The reason why the Fe(III)/Z-Ala-Gly-NHOH species stays in solution at such a high pH is not absolutely certain. However, it may be related to the possibly well shielded solution structure of the resulting tris(Z-Ala-Gly-NHOH)(Fe(III)) complex.

Kinetics

The dissociation kinetics of $[Fe(Z\text{-}Gly\text{-}NHO)]^{2+}$ has been investigated by stopped-flow method in a wide range of acid-concentration at a constant ionic strength of 1.0 and in the temperature range of 15–45 °C. The pseudo-first-order rate constants obtained are compiled in Table III as a function of perchloric acid concentration and temperature. A plot of observed dissociation rate constants against $[H^+]$ (Fig. 4) suggests that the decomplexation reaction undergoes by three parallel pathways. In the low-acid concentration range, the observed rate constants decrease with increase in $[H^+]$. At certain acidity, the rate-constant ceases to decrease and increases linearly with further increase in acid concentration. By extrapolating the rate constants in lower pH region one can get the value for acid-independent rate-constant (k_d).

The hydrolysis of $[Fe(H_2O)_6]^{3+}$ to yield $[Fe(H_2O)_5OH]^{2+}$ and H^+ is known to occur in aqueous solutions [19, 27]. Even after substituting one or more coordinated water molecules with neutral or anionic ligands, its tendency to hydrolyze still exists although diminished to certain extent due to the decrease in charge on the metal ion [18]. The resulting hydroxy species are more labile towards substitution or dissociation than the parent complex due to

TABLE III. Effect of Acidity on Dissociation Kinetics[a] of $[Fe\text{-}Z\text{-}Gly\text{-}NHO]^{2+}$

Temperature	k_{obs} (s^{-1}) at different $[H^+]$ (M)									
	2.5×10^{-3}	5×10^{-3}	1.25×10^{-2}	2.5×10^{-2}	5.0×10^{-2}	1.25×10^{-1}	2.5×10^{-1}	5.0×10^{-1}	7.5×10^{-1}	1.0
15	1.61×10^{-1}	1.03×10^{-1}	8.46×10^{-2}	7.05×10^{-2}	6.54×10^{-2}	6.34×10^{-2}	6.72×10^{-2}	7.41×10^{-2}	8.57×10^{-2}	9.97×10^{-2}
25	4.34×10^{-1}	3.33×10^{-1}	2.58×10^{-1}	2.07×10^{-1}	1.86×10^{-1}	1.72×10^{-1}	1.78×10^{-1}	1.98×10^{-1}	2.26×10^{-1}	2.42×10^{-1}
35	1.02	8.30×10^{-1}	6.45×10^{-1}	5.46×10^{-1}	4.95×10^{-1}	4.56×10^{-1}	4.51×10^{-1}	4.63×10^{-1}	5.03×10^{-1}	5.51×10^{-1}
45	2.21	1.36	1.15	1.08	1.02	1.02	9.72×10^{-1}	1.02	9.98×10^{-1}	1.01

[a][complex] = 2.0×10^{-4} M, μ = 1.0.

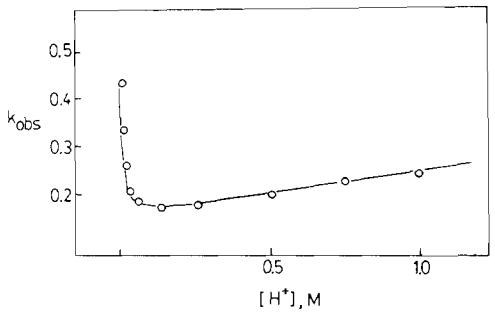

Fig. 4. Plot of k_{obs} *vs.* $[H^+]$ for $[Fe(Z\text{-}Gly\text{-}NHO)]^{2+}$ complex. ○: Experimental data points. Solid curve is the best fit according to the derived rate law (see text).

the strong labilizing effect of hydroxide ion. In the region where the decreasing trend in rate constants is seen with increase in acidity, the dominating species can be assigned as $[Fe(H_2O)_3(L)OH]^+$. With the increase in $[H^+]$, the equilibrium shifts towards left, thus decreasing the concentration of hydroxy species. The acid-catalyzed dissociation rate constant (k_H) though detectable is quite small as one would have anticipated. The cationic complex under study has a charge of +2 and through some degree of covalent bonding the charge could be dispersed from metal to ligating atoms. The electrophylic attack of proton on the coordinating atoms which generally is responsible for acid-catalyzed hydrolysis, is thus not very facile.

The acid-independent dissociation of complexes containing chelating ligands occurs by chelate ring-opening followed by the attack of a solvent molecule at the vacant coordination site [28]. This process can be assisted by acid through protonation of coordinating group immediately after ring-opening hence preventing the re-formation of chelate. The protonation of free coordinating atom is believed to be much faster than the ring opening and the latter stage therefore becomes the rate-determining step. This self-dissociation pathway contributes significantly in the dissociation of complex chosen for this study. The equilibrium constant for the reaction

$$[Fe(H_2O)_6]^{3+} + L^- \underset{k_d}{\overset{k_f}{\rightleftharpoons}} [Fe(H_2O)_4L]^{2+}$$

is $\sim 10^{11}$ M^{-1}. The formation rate constants [28, 29] for Fe(III) complexes are reported to be around 10^1 M^{-1} s^1. Assuming this value for k_f of our complex, the expected k_d can be calculated from the relation $k = k_f/k_d$, which is 10^{-10} s^{-1} and is nine orders of magnitude slower than the experimentally observed one at 25 °C. This indicates that as in other complexes containing polydentate ligands, the chelate ring-opening in our complex is the rate-determining step for the acid-independent dissociation pathway, as opposed to complete dissociation of ligand from the metal in one step.

TABLE IV. Resolved Rate and Hydrolysis Constants[a] for $[Fe\text{-}Z\text{-}GlyNHO]^{2+}$

Temperature (°C)	k_d (s^{-1})	k_H ($M^{-1}\,s^{-1}$)	K_h (M)
15	$(5.8 \pm 0.3) \times 10^{-2}$	$(3.77 \pm 0.52) \times 10^{-2}$	
25	$(1.53 \pm 0.05) \times 10^{-1}$	$(8.92 \pm 0.84) \times 10^{-2}$	$(2.76 \pm 0.55) \times 10^{-3}$
35	$(4.09 \pm 0.10) \times 10^{-1}$	$(1.2 \pm 0.16) \times 10^{-1}$	$(3.68 \pm 0.57) \times 10^{-3}$

[a]From observed rate constants shown in Table III.

The reaction scheme incorporating all the available pathways can be written as follows:

$$FeL^{2+} \underset{k_{-d}}{\overset{k_d}{\rightleftharpoons}} [FeL^{2+}]^* \xrightarrow[\text{fast}]{H_2O/H^+} Fe^{3+} + HL$$

$$FeL^{2+} + H^+ \xrightarrow{k_H} Fe^{3+} + HL$$

$$Fe(L)H_2O^{2+} \overset{K_h}{\rightleftharpoons} Fe(L)OH^+ + H^+$$

$$Fe(L)OH^+ \xrightarrow{k_{-H}} FeOH^{2+} + L/HL$$

The rate-law derived from the proposed mechanism comes out to be

$$\frac{-d[\text{complex}]}{dt} = \frac{k_d + K_h - k_{-H}[H^+]^{-1} + k_H[H^+]}{1 + K_h[H^+]^{-1}}[\text{complex}]$$

The real rate constants for the self-dissociation (k_d), and acid catalyzed (k_H) rate constant and the hydrolysis constant (K_h) have been resolved by non-linear regression analysis of observed pseudo-first-order rate constants (k_{obs}) and are given as a function of temperature in Table IV. The rate-data at 45 °C are not accurate enough to resolve all the rate constants. The hydrolysis constant (K_h) obtained from the rate-data at 25 °C and 1.0 μ, is very close to the reported value [19, 30] for $[Fe(H_2O)_6]^{3+}$ under similar conditions. The tendency of hydrated Fe^{3+} to hydrolyze is thus not diminished even after the incorporation of hydroxamic acid into the coordination sphere of this metal ion, contrary to earlier observations by other workers [31]. Kinetic measurements done at 25 °C and 1.0 M $[H^+]$ varying [electrolyte] from 1.0 to 4.0 M suggest that the dissociation rate of the complex under study, is not influenced by the amount of electrolyte in the reaction mixture. The observed rate-constants obtained under the aforementioned conditions, are within experimental error, *i.e.* $(2.25 \pm 0.11) \times 10^{-1}\,s^{-1}$.

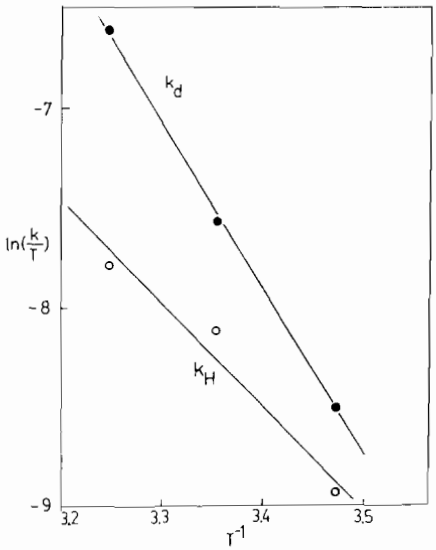

Fig. 5. Plots of $\ln(k_d/T)$ and $\ln(k_H/T)$ *vs.* $1/T$ for $[Fe(Z\text{-}Gly\text{-}NHO)]^{2+}$ complex.

The activation parameters obtained from the plots of $\ln(k_d/T)$ and $\ln(k_H/T)$ against T^{-1}, Fig. 5, for self-dissociation and acid-dependent pathways are $\Delta H_d^{\neq} = 16.6 \pm 0.4$ kcal/mol, $\Delta S_d^{\neq} = -6.5 \pm 1.3$ e.u.; $\Delta H_H^{\neq} = 10.2 \pm 2.4$ kcal/mol and $\Delta S_H^{\neq} = -29.6 \pm 8.0$ e.u. (The error limits quoted represent one standard deviation). These values are very much consistent with proposed reaction pathways and are in excellent agreement with those previously reported for other Fe(III)–hydroxamic acid complexes [30]. The higher $\Delta H_d^{\neq}$ values as compared to $\Delta H_H^{\neq}$ is expected because more energy is needed to open the chelate-ring as compared to bond-formation between H^+ and ligand nitrogen. A large negative $\Delta S_H^{\neq}$ also points towards a concerted process.

Acknowledgements

We acknowledge financial support by NIH-MBRS Grant No. 5-S06 RR08012-15 (CAC) and 5-S06-RR08136-11 (FSG) and by U.S. Department of Energy Grant No. DE-FG05-84ER13292 (CAC). We also thank Lynn J. San Filippo for assistance in spectroscopic characterizations of key compounds.

References

1 N. Nishino and J. C. Powers, *Biochemistry, 17,* 2846 (1978).
2 D. Rasnick and J. C. Powers, *Biochemistry, 17,* 4363 (1978).
3 N. Nishino and J. C. Powers, *J. Biol. Chem., 255,* 3482 (1980).
4 J. O. Baker, S. H. Wilkes, M. E. Bayliss and J. M. Prescott, *Biochemistry, 22,* 2098 (1983).
5 S. H. Wilkes and J. M. Prescott, *J. Biol. Chem., 258,* 13517 (1983).
6 D. A. Brown and M. V. Chidambaram, in H. Sigel (ed.), 'Metal Ion in Biological Systems', Vol. 14, Marcel Dekker, New York, 1982, p. 125.
7 K. N. Raymond, *Adv. Chem. Ser., 162,* 33 (1977).
8 J. B. Neilands, *Adv. Chem. Ser., 162,* 3 (1977).
9 J. B. Neilands, 'Microbial Iron Metabolism', Academic Press, New York, 1974.
10 J. B. Neilands, in G. Eichhorn (ed.), 'Inorganic Biochemistry', American Elsevier, New York, 1973, Chap. 5.
11 T. Emery, in H. Sigel (ed.), 'Metal Ions in Biological Systems', Vol. 7, Marcel Dekker, New York, 1978, p. 77.
12 J. H. Weisburger and E. K. Weisburger, *Pharm. Rev., 25,* 1 (1973).
13 O. Mikes and T. Turkova, *Chem. Listy, 58,* 65 (1964).
14 R. T. Coults, *Can. J. Pharm. Sci., 2,* 27 (1967).
15 J. B. Neilands, *Science, 156,* 1443 (1967).
16 H. Maehr, *Pure Appl. Chem., 28,* 603 (1971).
17 K. N. Raymond, G. Muller and B. F. Matzanke, *Top. Curr. Chem., 123,* 49 (1984).
18 S. A. Kazmi and J. A. McArdle, *J. Inorg. Nucl. Chem., 43,* 3031 (1980).
19 E. Mentasti, F. Secco and M. Venturini, *Inorg. Chem., 21,* 602 (1982).
20 C. A. Chang and M. E. Rowland, *Inorg. Chem., 22,* 3866 (1983).
21 C. A. Chang and V. O. Ochaya, *Inorg. Chem., 25,* 355 (1986).
22 E. Hoffman and I. Faiferman, *J. Org. Chem., 29,* 748 (1964).
23 H. Irving and H. S. Rosotti, *J. Chem. Soc.,* 2904 (1954).
24 J. C. Sullivan, J. Rydberg and W. F. Miller, *Acta Chem. Scand., 13,* 2023 (1959).
25 W. A. E. McBryde, *Can. J. Chem., 42,* 1917 (1964).
26 W. A. E. McBryde and G. F. Atkinson, *Can. J. Chem., 39,* 510 (1961).
27 J. H. Espenson and R. C. McHatton, *Inorg. Chem., 20,* 3090 (1981).
28 D. W. Margerum, G. R. Cayley, D. C. Weatherburn and G. K. Pagenkopf, *Am. Chem. Soc. Monogr., 174,* 1 (1978) and refs. therein.
29 K. Kustin and J. Swinehart, *Prog. Inorg. Chem., 13,* 107 (1970) and refs. therein.
30 B. Monzyk and A. L. Crumbliss, *J. Am. Chem. Soc., 101,* 6203 (1979).
31 B. S. Prabhananda, *J. Inorg. Nucl. Chem., 40,* 525 (1978).
32 A. E. Martell and R. M. Smith, 'Critical Stability Constants', Vol. 3, Plenum, New York, 1974, p. 301.